iScience

CellPress
OPEN ACCESS

Article

LY-2183240 enhances reward-seeking behavior with inducing neuronal excitation and early apoptosis in mouse

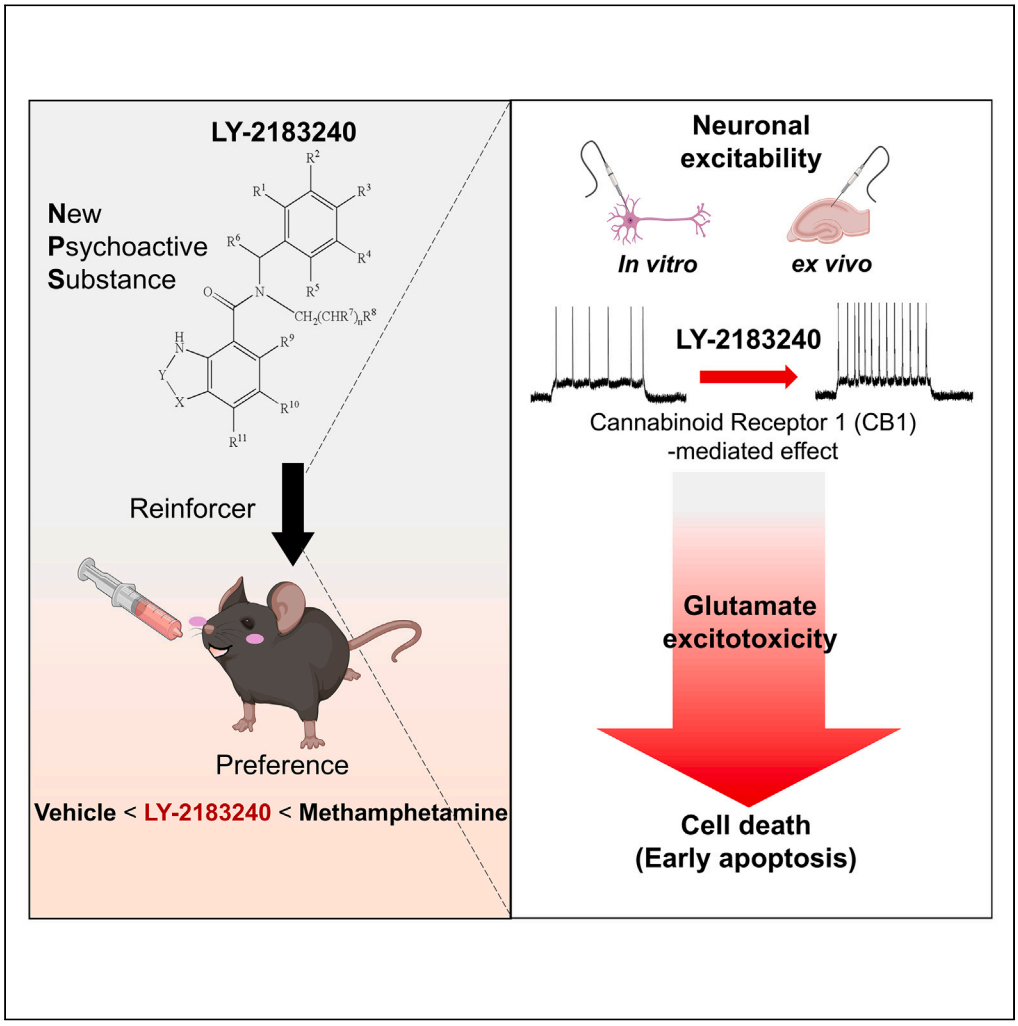

Yu Yeong Jeong, Jae Hong Yoo, Seo Yule Jeong, ..., Seung Won Son, Kyung-Seok Han, Dong Ho Woo

kshan711@cnu.ac.kr (K.-S.H.)
dongho.woo@kitox.re.kr (D.H.W.)

Highlights

LY-2183240, a new psychoactive substance, induces neuronal excitability *in vitro* and *ex vivo*

LY-2183240 causes glutamate excitotoxicity and induces early apoptosis

LY-2183240 acts as a reinforcer, which may indicate some potential for abuse

Jeong et al., iScience *27*, 111069
November 15, 2024
https://doi.org/10.1016/j.isci.2024.111069

iScience

CellPress
OPEN ACCESS

Article

LY-2183240 enhances reward-seeking behavior with inducing neuronal excitation and early apoptosis in mouse

Yu Yeong Jeong,[1,3,5] Jae Hong Yoo,[3,5] Seo Yule Jeong,[1] Myunghoon Lee,[3] Su Jeong Park,[4] Na Young Lim,[4] Seung Won Son,[4] Kyung-Seok Han,[3,*] and Dong Ho Woo[1,2,6,*]

SUMMARY

Cannabinoids interact with cannabinoid receptors, influencing diverse central nervous system (CNS) and peripheral functions, including anxiety, depression, and cognition. CB1 and CB2 receptors modulate signaling cascades via G-protein coupling, with anandamide acting as an endogenous ligand for CB1 receptors. LY-2183240, a putative endocannabinoid transport blocker, elevates brain anandamide levels, showing therapeutic potential in pain management and alcohol-related behaviors. LY-2183240 enhances neuronal excitability and is classified as a new psychoactive substance (NPS). However, its precise cellular mechanisms within the CNS remain poorly understood. In this study, the effect of LY-2183240 on cortical neurons and reward-seeking behavior is investigated. Our results indicate enhanced neuronal excitability and reward-seeking behavior induction by LY-2183240, shedding light on its pharmacological profile and NPS-associated risks. Our research underscores the importance of further understanding the cellular mechanisms of LY-2183240 to inform regulatory efforts and mitigate public health risks.

INTRODUCTION

Cannabinoids are commonly defined as compounds that interact with cannabinoid receptors, alongside chemically related substances. The cannabinoid system exerts its influence on both central nervous system (CNS) and peripheral processes by modulating various functions such as anxiety, depression, neurogenesis, reward processing, cognition, learning, and memory.[1] Notably, CB1 and CB2 serve as the primary cannabinoid receptors. These receptors couple to G-proteins, particularly Gi/o, and can trigger various signaling cascades, including the inhibition of adenylyl cyclase. Anandamide is a lipid mediator that functions as an endogenous ligand of CB1 receptors.[2] Based on preclinical data, compounds that inhibit the cellular accumulation of anandamide exhibit significant therapeutic potential for treating multiple sclerosis, pain management, and cancer.[3,4] Extracellular anandamide is eliminated through a process involving cellular uptake followed by metabolism.

LY-2183240, also referred to as 5-(4-biphenylylmethyl)-N,N-dimethyl-1H-tetrazole-1-carboxamide, is known as a putative endocannabinoid transport blocker.[5,6] Administering LY-2183240 to rats increases anandamide levels in the brain, effectively reducing pain without affecting motor performance.[7] This suggests that inhibitors targeting anandamide transport could offer valuable therapeutic benefits. Studies have demonstrated that repeated administration of LY-2183240 decreased the expression of fear-potentiated startle in subjects with a high preference for alcohol and, the application of LY-2183240 increased conditioned place preference (CPP) induced by alcohol.[8] LY-2183240 interacting with endocannabinoid system showed antiepileptic effects in mice.[9] The structure of LY-2183240 is similar to that of specific fatty acid amide hydrolase (FAAH) inhibitors, which hydrolyses the endocannabinoid to arachidonic acid and ethanolamine,[10] thus it also known as potent inhibitor of FAAH both *in vitro* and *in vivo*.[11] LY-2183240 has been observed to enhance neuronal excitability in rat primary cortical neurons.[12] It is also classified among the recently distributed designer drugs.[13] Nevertheless, the specific cellular mechanisms and functions of LY-2183240 within the CNS remain largely unexplored.

New psychoactive substances (NPSs) refer to designer or synthetic drugs marketed under various names such as "legal high products," "bath salts," and "research chemicals."[14,15] These substances, as defined by the United Nations Office for Drugs and Crime (UNODC), are characterized as "substances of abuse, whether in their pure form or as preparations, that are not regulated by the 1961 Single Convention

[1]Center for Global Biopharmaceutical Research Korea Institute of Toxicology, KRICT, Daejeon 34114, South Korea
[2]Human and Environmental Toxicology, University of Science and Technology, Daejeon 34114, South Korea
[3]Department of Biological Sciences, Chungnam National University, Daejeon 34134, South Korea
[4]Pharmacology and Narcotics Research Division, National Institute of Food & Drug Safety Evaluation, Cheongju-si, South Korea
[5]Senior authors
[6]Lead contact
*Correspondence: kshan711@cnu.ac.kr (K.-S.H.), dongho.woo@kitox.re.kr (D.H.W.)
https://doi.org/10.1016/j.isci.2024.111069

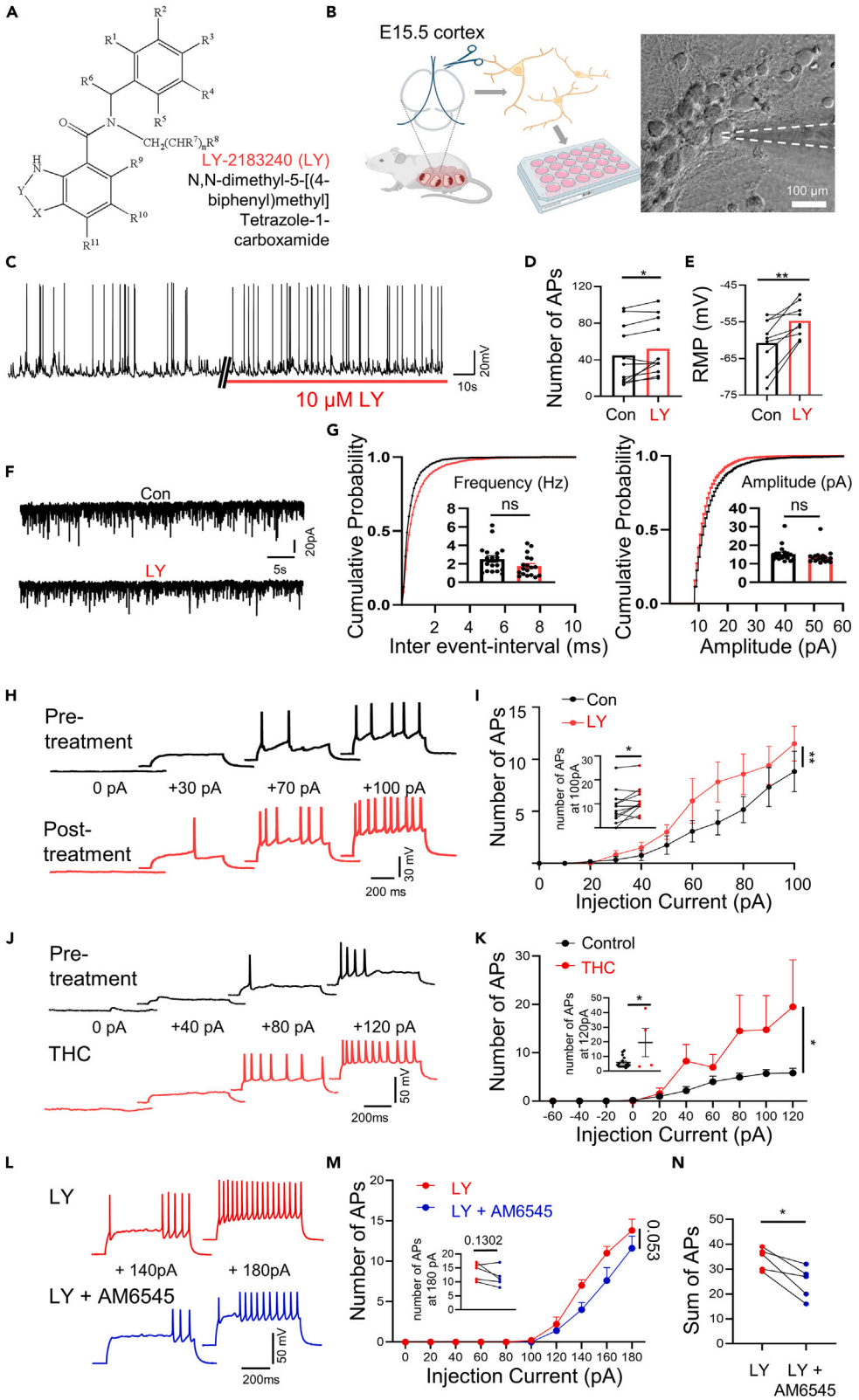
A
LY-2183240 (LY)
N,N-dimethyl-5-[(4-biphenyl)methyl]
Tetrazole-1-carboxamide
B
E15.5 cortex
100 μm
C
10 μM LY
20mV
10s
D
Number of APs
Con
LY
E
RMP (mV)
Con
LY
F
Con
LY
20pA
5s
G
Cumulative Probability
Frequency (Hz)
ns
Inter event-interval (ms)
Amplitude (pA)
ns
Amplitude (pA)
H
Pre-treatment
0 pA
+30 pA
+70 pA
+100 pA
Post-treatment
30 mV
200 ms
I
Con
LY
Number of APs
number of APs at 100pA
Injection Current (pA)
J
Pre-treatment
0 pA
+40 pA
+80 pA
+120 pA
THC
50 mV
200ms
K
Control
THC
Number of APs
number of APs at 120pA
Injection Current (pA)
L
LY
+ 140pA
+ 180pA
LY + AM6545
50 mV
200ms
M
LY
LY + AM6545
Number of APs
number of APs at 180 pA
0.1302
0.053
Injection Current (pA)
N
Sum of APs
LY
LY + AM6545

Figure 1. LY-2183240 excites mouse cortical-cultured neurons

(A) The structure of LY-2183240 (LY).

(B) Schematic image of primary neuron culture (left) and differential interference contrast (DIC) image (right) with patch pipette (white dot line).

(C) Representative traces of action potential before (left) and after (right) LY application (red bar).

(D and E) Summary graphs of (D) number of APs (paired t tests, $*p = 0.0227$) and (E) resting membrane potential (RMP) (paired t tests, $**p = 0.0035$).

(F) Representative traces for mEPSCs recorded at cultured neurons.

(G) Cumulative probability plots of mEPSC inter-event interval and amplitude. Averaged frequency and amplitude are shown in the inner bar graph (unpaired t tests, ns, $p > 0.05$).

(H) Representative AP traces in control and LY application neurons.

(I) Measuring number of APs evoked by step current injection in control and LY application neurons (paired t test, $**p = 0.0056$). Number of APs at 100 pA injection is shown in the inner bar graph (paired t tests, $*p = 0.020$).

(J) Representative voltage traces in the current clamp mode before the treatment (upper, black trace) and during the treatment with 30 μM tetrahydrocannabinol (lower, red trace).

(K) Measuring number of APs evoked by step current injection in control and THC application neurons (paired t tests, $*p = 0.0288$). Number of APs at 120 pA injection is shown in the inner bar graph (unpaired t test, $*p = 0.011$).

(L) Representative voltage traces in the current clamp mode before the treatment (upper, red trace) and during the treatment with LY-2183240 and 10 μM AM6545, a CB1 receptor antagonist (lower, blue trace).

(M) Measuring number of APs evoked by step current injection in LY application and LY with antagonist neurons (paired t tests, ns, $p = 0.053$). Number of APs at 180 pA injection is shown in the inner bar graph (unpaired t test, ns, $p = 0.130$).

(N) The plot represents the cumulative value of all APs that occurred during the current step (paired t tests, $*p = 0.017$). Data are represented as mean ± SEM.

on Narcotic Drugs or the 1971 Convention on Psychotropic Substances, but which may present a public health risk."[15–19] The rapid evolution of NPSs poses a significant threat to public health, as their structures change swiftly.[20] Despite their involvement in criminal activities, the lack of scientific evidence complicates national efforts to regulate these substances effectively. Therefore, it is important to conduct experimental research to establish a solid scientific basis for national regulation.

NPSs are known to influence synaptic transmission in the brain, leading to behavioral changes.[19,21–23] In this study, we examine the effect of LY-2183240 at cellular level and reward-seeking behavior. Our findings reveal that LY-2183240 enhances intrinsic excitability by elevating the frequency of action potentials (APs) in cortical neurons, without affecting intracellular Ca^{2+} responses. Furthermore, LY-2183240 treatment leads to an increase in extracellular glutamate concentration, which subsequently results in a reduction in the number and processes of neurons. Additionally, through self-administration (SA) and CPP tests, we demonstrate that LY2183240 induces reward-seeking behavior. This study elucidates the cellular mechanisms and the functional implications of LY-2183240 at both cellular and behavioral levels.

RESULTS

LY-2183240 excites excitatory mouse cortical neurons

LY-2183240, distinguished by its heteroaryl carboxamide framework, exerts influence on the CNS and is compared to synthetic cannabis. While it functions as an inhibitor of anandamide reuptake and fatty acid amid hydrolase, the direct physiological effects induced in the brain have yet to be identified. To evaluate the effect of LY-2183240 on the intrinsic excitability of neurons, we conducted *in vitro* whole-cell patch clamp recordings on cortical neurons from days 12–14 after initiating a primary culture using the cortex of C57BL/6 embryos (Figure 1B). The application of 10 μM of LY-2183240 resulted in an increase in the number of spontaneous action potentials (sAPs) (Figures 1C and 1D). Additionally, we observed an elevation in the resting membrane potential (RMP) induced by LY-2183240 (Figure 1E). To evaluate the effect of LY-2183240 on non-AP-mediated synaptic transmission such as astrocyte effects and non-AP-mediated presynaptic effect, we recorded miniature excitatory postsynaptic currents (mEPSCs). The mEPSC recordings were preceded by the inhibition of the voltage-gated Na^+ channel with 1 μM tetrodotoxin (TTX) (Figure 1F). Non-significant changes in both average frequency and amplitude before and after LY-2183240 treatment (Figure 1G) suggesting that the increased APs induced by LY-2183240 are not associated with synaptic function. Subsequently, to investigate the response of AP through current injection, we employed the current clamp technique to quantify the count of APs both before and after treatment. In the presence of LY-2183240, an increase in the number of APs was observed throughout most of the gradual current injection (Figures 1H and 1I). These results indicate that LY-2183240 increases intrinsic neuronal excitability without affecting synaptic transmission.

To confirm whether this effect of LY-2183240 occurs within tissue, we conducted whole-cell patch clamp recordings in the CA1 region of the hippocampus following a horizontal section of the mice's brain (Figures 2A and 2B). In the acute brain slice, we observed an increase in the AP generated by current injection in the presence of LY-2183240 (Figure 2D). Additionally, we confirmed overall rise in the number of APs at each current step (Figure 2E). LY-2183240 demonstrated a consistent effect in both *in vitro* and *ex vivo* settings.

LY-2183240 is associated with the CB1 receptor

We hypothesized that LY-2183240 modulates the CB1 receptor, resulting in an increase in AP. To validate this effect, we treated 30 μM tetrahydrocannabinol (THC, IUPAC name (6aR,10aR)-6,6,9-trimethyl-3-pentyl-6a,7,8,10a-tetrahydrobenzo[c]chromen-1-ol), a CB1 agonist, and observed a similar increase in AP as seen with LY-2183240 (Figures 1J and 1K). Interestingly, LY-2183240-mediated excitability was reduced by AM6545, a specific CB1 antagonist (Figures 1L–1N). These findings suggest that LY-2183240 modulates the CB1 receptor, consequently leading to an increase in AP.

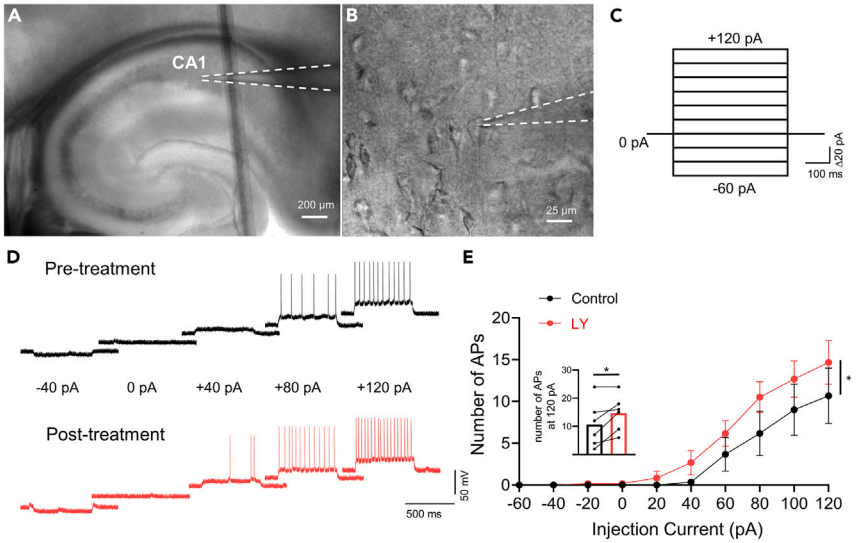

Figure 2. LY-2183240 excites hippocampal CA1 pyramidal neurons of C57BL/6 mice

(A) Bright field image showing a glass pipette above the hippocampal CA1 region. Scale bar: 200 μm.

(B) High-magnification image showing a glass pipette used for the whole-cell patch-clamp recording of CA1 pyramidal neurons. Scale bar: 25 μm.

(C) A series of current steps 20 pA increments was delivered (holding potential −70 mV) from −60 pA to +120 pA for 1s (scale bar: 20 pA and 100 ms).

(D) Representative voltage traces in the current clamp mode before the treatment (upper, black trace) and during the treatment with 10 μM LY-2183240 (lower, red trace).

(E) Plot comparing the numbers of APs recorded during a 0.6 s current application using the current step protocol (black indicates before the 10 μM LY-2183240 treatment; red indicates during the 10 μM LY-2183240 treatment). Summary bar graph comparing the numbers of APs recorded before and during the treatment with LY-2183240 (paired t test, $*p = 0.01$). Number of APs at 120 pA injection is shown in the inner bar graph (paired t test, $*p = 0.035$). Data are represented as mean ± SEM.

LY-2183240 increases extracellular glutamate release

To ascertain whether the rise in APs induced by LY-2183240 is linked to an elevation in intracellular metabotropic Ca^{2+} level within neuronal cytoplasm, we conducted calcium imaging in the primary cultured cortical neurons (Figure 3A). Initially, the augmentation of intracellular calcium was validated through treatment with glutamate and glycine (Figure 3B). However, no discernible calcium response was observed by the treatment of LY-2183240 (Figure 3B). These findings suggest that LY-2183240 dose not lead to an elevation in APs associated with an increase in intracellular metabotropic Ca^{2+} that is related non AP-mediations and astrocyte effects.

Considering that an increase in APs could potentially trigger more neurotransmitter release and influence the resulting glutamate concentration in the synapse, we measured the glutamate concentration in the neuronal medium treated with 0.1% DMSO, 10 μM LY-2183240, and 100 μM LY-2183240 (Figure 3C). We simultaneously treated hyperosmotic solutions (530 mOsm/kg) to induce changes in ionic balance by triggering cellular responses aimed at osmotic regulation and ultimately promoting the release of the neurotransmitter glutamate as a positive control. Subsequently, we collected the medium 1 and 20 h later to proceed with the glutamate assay. Under incubation conditions of 1 and 20 h, LY-2183240 demonstrated a significant elevation in glutamate levels at both concentrations. Notably, treatment with 100 μM LY-2183240 revealed higher concentrations of glutamate compared to treatment with a hyperosmotic solution (Figure 3D).

LY-2183240 devastates cortical neurons by inducing early apoptosis

We investigated the effect of LY-2183240 on cell death and the morphology in primary cultured cortical neurons for 24 and 72 h. In cell viability assays, we observed that LY-2183240 induces neuronal death, with an IC_{50} of 6.9 μM (Figures 4A–4C). Using cultured neurons, we conducted NeuN and microtubule-associated protein 2 (MAP2) staining to know whether LY-2183240 disrupts neuronal processes meaning neuronal functions such as synaptic transmission and intrinsic property. The expression of NeuN and MAP2 has been observed across various regions of the rodent nervous system, encompassing the medulla, cerebellum, pons, midbrain, caudate putamen, septum, hypothalamus, piriform cortex, amygdala, parietal cortex and more. The expression of NeuN and MAP2 was examined in the untreated control group and in groups treated with 10 μM LY-2183240 for 24 and 72 h. (Figure 4D). Treatment with 10 μM LY-2183240 for 24 and 72 h significantly reduced the total DAPI number (Figure 4E), DAPI + NeuN number (Figure 4F), and MAP2 intensity (Figure 4G) compared to the control group. Based on the decrease in the number of cells induced by LY-2183240, we conducted flow cytometry for neurotoxicity assessment to investigate how LY-2183240 causes cell death. We performed flow cytometry analysis using annexinV and propidium iodide (PI) staining to determine whether the death mechanism is through apoptosis and necrosis (Figure 5A). The treatment of 10, 50, and 100 μM LY-2183240 reduced cell viability

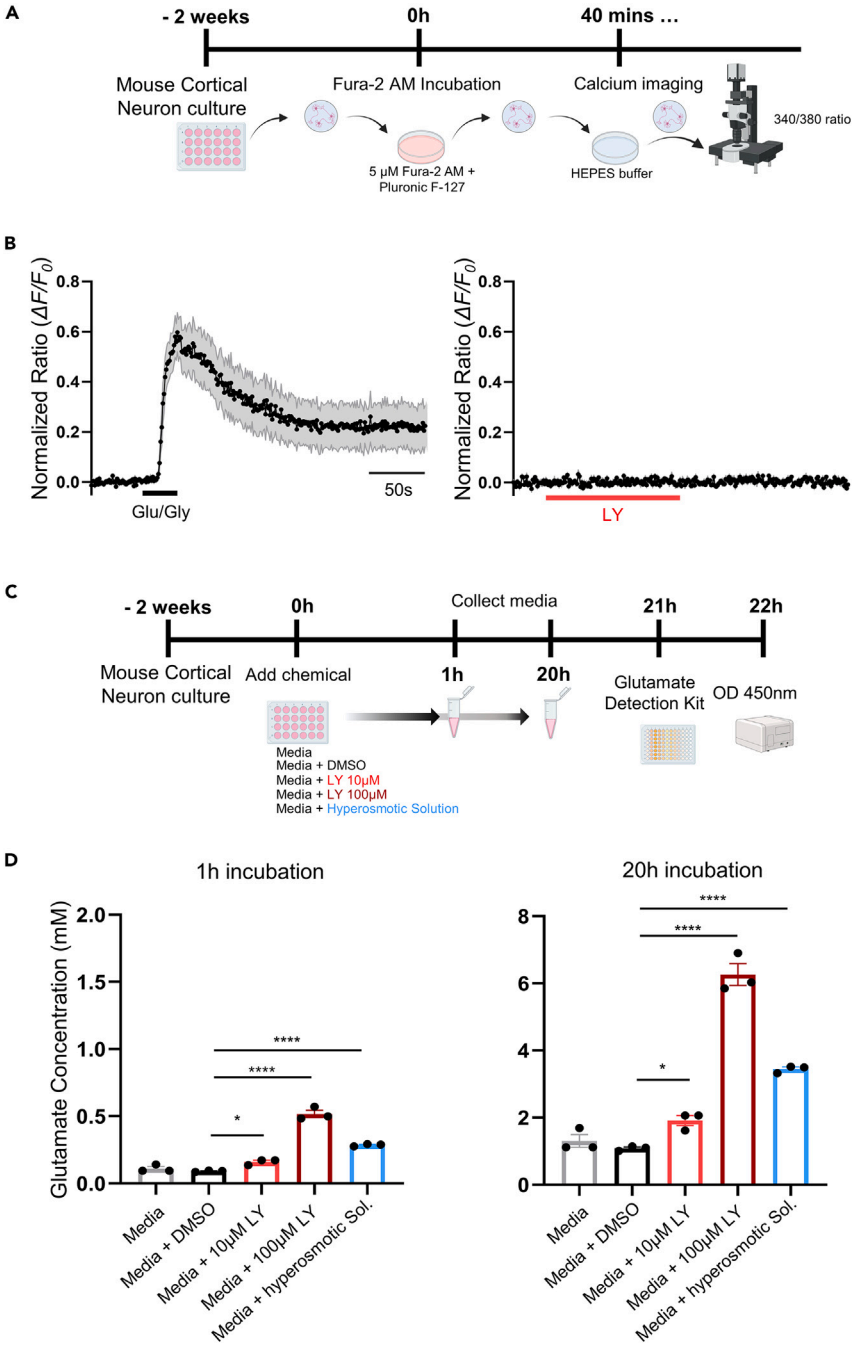

Figure 3. LY-2183240 increases extracellular glutamate concentration without Ca^{2+} dependency

(A) Experimental timeline of calcium imaging.

(B) Representative normalized ratio trace (ΔF/Fo) showing response of calcium imaging to Glu/Gly (left) and 10 μM LY-2183240 (right) in primary cultured rat neurons.

(C) Experimental timeline of glutamate assay. We proceeded by adding the drug to 1 mL of media per well so that the final concentration of LY was 10 μM and 100 μM.

(D) Summarized bar graph of glutamate concentration for LY-2183240 incubated for 1 h (left) and 20 h (right) (one-way ANOVA: $F(4,10) = 0.5664$, Dunnett's multiple comparisons test $^*p = 0.031$ and $^{****}p < 0.0001$, $n = 3$). Data are represented as mean ± SEM.

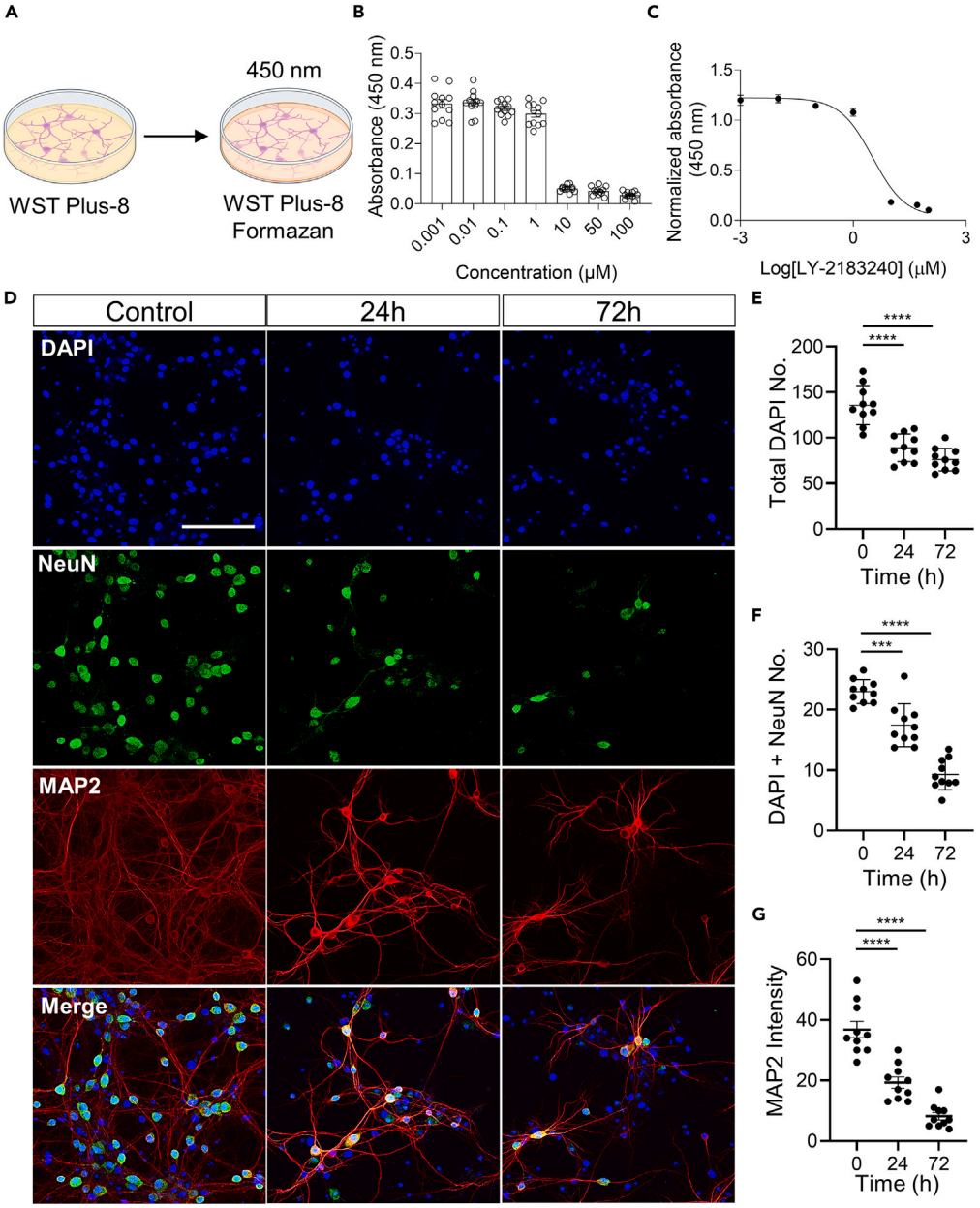

Figure 4. LY-2183240 devastates mouse cortical neurons by the reductions both of neuronal cell number and arborization

(A) The scheme of CCK-8 assay.

(B) Summarized bar graph of absorbance at 450 nm for LY-2183240 in manner of dose dependency (n = 12).

(C) Inhibitory concentration of LY-2183240 on primary neurons. IC_{50} = 6.91 μM.

(D) Representative fluorescent images showing primary cultured mouse neurons of treated 10 μM LY-2183240 time dependent. Nuclei were stained with DAPI(blue). NeuN(green) indicates neuronal nuclear. MAP2(red) indicates neuronal dendrites and merged image. Control (left), 24 h (middle) and 72 h (right) treatment of 10 μM LY-2183240. Scale bar: 100 μm.

(E and F) Bar graphs summarizing the number of (E) total DAPI and (F) DAPI+ NeuN+ (one-way ANOVA: F(2,27) = 0.8424, p = 0.001, Dunnett's multiple comparisons test ***p < 0.001 and ****p < 0.0001).

(G) Bar graph summarizing the MAP2 intensity (one-way ANOVA: F(2,27) = 1.629, p = 0.001, Dunnett's multiple comparisons test ****p < 0.0001), (n = 10). Data are represented as mean ± SEM.

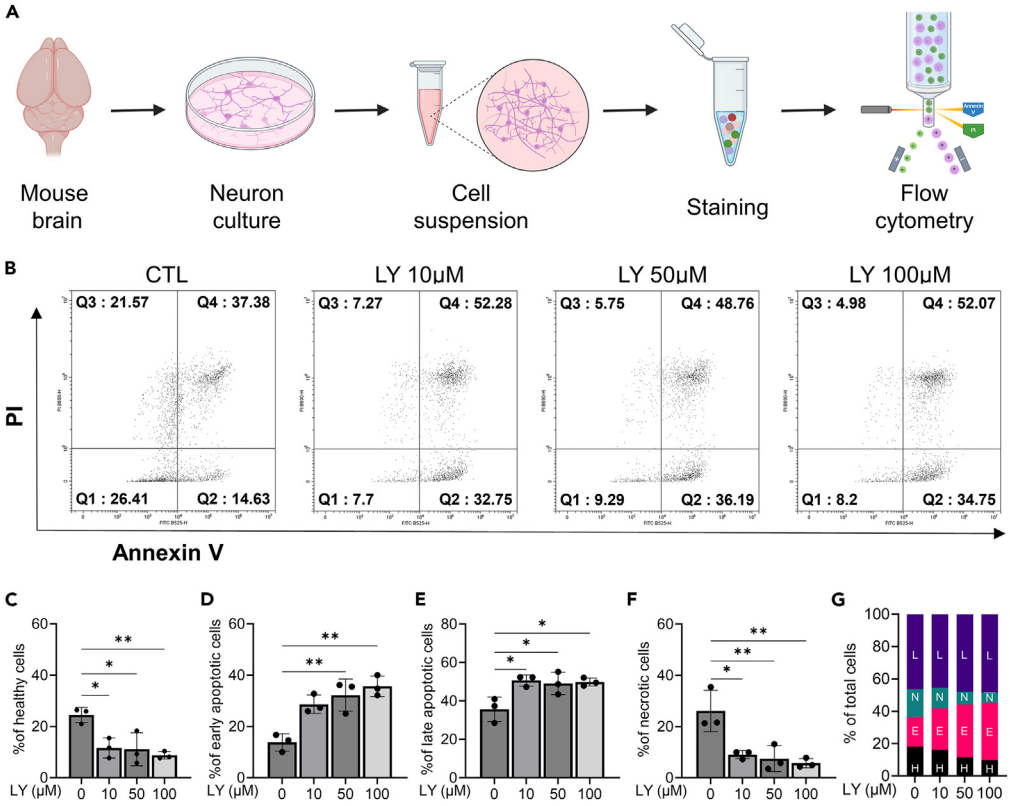

Figure 5. LY-2183240 induces early apoptosis of primary cultured mouse neurons

The lines for quadrants indicate cortical neurons without staining annexin V and PI. Representative scatterplots of the distribution of CTL(LY-2183240 0 μM), LY-2183240 10 μM, LY-2183240 50 μM, and LY-2183240 100 μM treatments. During flow cytometry, the lower left quadrant contained healthy cells (Q1; annexin V−, PI−), the upper left quadrant had dead cells (Q3; necrotic cells; annexin V−, PI+), the upper right quadrant had late apoptotic cells (Q4; annexin V+, PI+), and the lower right quadrant contained early apoptotic cells (Q2; annexin V+, PI−).

(A) Workflow diagram depicting the flow cytometry protocol.

(B) Representative quadrant in flow cytometry. Early apoptosis is Q2 in each quadrant.

(C–F) Summary bar graphs, (C) % of healthy cells (Q1, one-way ANOVA: $F(3,8) = 8.850$, $p < 0.05$ Tukey post hoc test $^{*}p < 0.05$, LY-2183240 0 μM & LY-2183240 10 μM, LY-2183240 0 μM & LY-2183240 50 μM, $^{**}p < 0.01$, LY-2183240 0 μM & LY-2183240 100 μM), (D) % of early apoptotic cells (Q2, one-way ANOVA: $F(3,8) = 13.92$, $p < 0.05$ Tukey post hoc test $^{**}p < 0.01$, LY-2183240 0 μM & LY-2183240 10 μM, LY-2183240 0 μM & LY-2183240 50 μM), (E) % of late apoptotic cells(Q4, one-way ANOVA: $F(3,8) = 6.993$, $p < 0.05$ Tukey post hoc test $^{*}p < 0.05$, LY-2183240 0 μM & LY-2183240 10 μM, LY-2183240 0 μM & LY-2183240 50 μM, LY-2183240 0 μM & LY-2183240 100 μM), and (F) % of necrotic cells (Q3, one-way ANOVA: $F(3,8) = 11.05$, $p < 0.05$ Tukey post hoc test $^{*}p < 0.05$, LY-2183240 0 μM & LY-2183240 10 μM, $^{**}p < 0.05$ LY-2183240 0 μM & LY-2183240 50 μM, LY-2183240 0 μM & LY-2183240 100 μM).

(G) Summary graph for LY-2183240 treatment (L, late apoptotic cells; N, necrotic cells; E, early apoptotic cells; H, healthy cell). Data are represented as mean ± SEM.

(Figures 5B and 5C) by inducing early apoptosis (Figure 5D), subsequently late apoptosis was increased (Figure 5E). As a result, necrosis was significantly reduced (Figure 5F). These results demonstrate that 10 μM LY-2183240 induced early apoptosis (Figure 5G). 50 and 100 μM LY-2183240 no longer significantly increase early apoptosis than 10 μM, suggesting that LY-2183240 induces 15% early apoptosis in average of certain neuronal population.

LY-2183240 increases the infusion volume for SA

So far, our results have shown that the cellular mechanism of LY-2183240 increases excitability, abnormally increases extracellular glutamate release in neurons, and provides 15% in average early apoptosis of neuronal population. There is no scientific evidence for dependence on LY-2183240. So we performed SA to see if LY-2183240 acts as a reinforcer that may indicate some potential for abuse. *In vivo*, SA represents a type of operant conditioning in which drug consumption serves as the reward. Mice undergoing chronic intravenous (i.v.) drug SA represent a valuable method for predicting the abuse potential of new drugs in humans, assessing potential treatments for drug abuse and dependence, and investigating the biological mechanisms underlying addiction.[24] LY-2183240 SA was performed in standard operant chambers once daily. While tethered to an infusion syringe via their dorsal catheter port, each mouse was afforded the freedom to move within the operant chamber. A cue light inside the chamber indicated the start of each SA and the lever available for manipulation (Figure 6A). The infusion

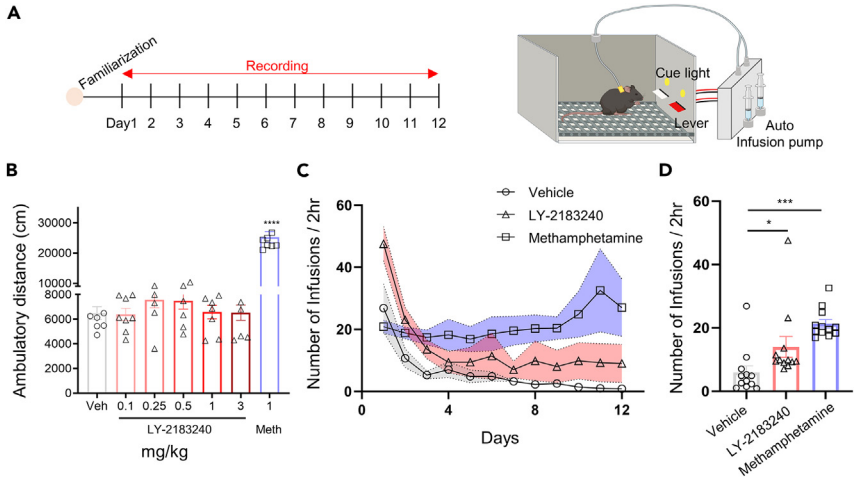

Figure 6. Intravenous (i.v.) injection of 0.05 mg/kg LY-2183240 for 12 days increases pushing frequency of active lever and infusion volume for self-administration (SA)

(A) Timeline for drug SA (left) and schematic diagram(right).

(B) Mice were injected with vehicle, LY-2183240 (0.1, 0.25, 0.5, 1, and 3 mg/kg) and Meth (1 mg/kg). The effects of LY-2183240 on the total ambulatory distances traveled was measure over 60 min ****$p < 0.0001$ compared to the vehicle group (one-way ANOVA: $F(6,49) = 1.111$, $p = 0.001$, Dunnett's multiple comparison test, ****$p < 0.0001$ $n = 5–8$).

(C) 1 lever pressing infuses 10 μL saline, 0.05 mg/kg LY2183240 and 0.01 mg/kg methamphetamine for 2 h.

(D) Summary bar graph for averaged number of lever pressing values in 12 days (one-way ANOVA: $F(2,33) = 0.2656$, $p = 0.01$, Dunnett's multiple comparisons test. *$p = 0.041$ saline versus LY2183240 and ***$p = 0.0001$ saline versus methamphetamine, $n = 12$). Data are represented as mean ± SEM.

of LY-2183240 did not show any significant difference but tended to increase ambulatory distance in a dose-dependent manner (Figure 6B). Compared to the control, both 0.05 mg/10 μL/kg LY-2183240 and 0.01 mg/10 μL/kg methamphetamine showed significant differences in infusion bar pressing for 12-day training (Figures 6C and 6D). When single bar pressing releases 10 μL, and LY-2183240 caused the mouse to press the lever 15 times on average per day, in contrast to 20 times on average in methamphetamine (Figures 6C and 6D). The average volumes per day of SA were 150 μL for LY-2183240 and 200 μL for methamphetamine, corresponding to average daily doses of 2.43 and 1.34 μM, respectively. This results in cumulative doses of 17.01 and 9.38 μM over the course of 7 days of injection. These amounts are comparable to the 10 μM concentration used *in vitro*, thereby reinforcing the connection between our *in vitro* and *in vivo* results. These findings suggest that although LY-2183240 is weaker than methamphetamine, it has potential drug with addiction-like behavior.

LY-2183240 alters dwelling time in both preference and non-preference place

We conducted CPP as one of the tests to evaluate the psychological dependence of LY-2183240. CPP arises when a mouse forms a preference for a specific location over others due to its prior association with rewarding stimuli.[25] Using the CPP apparatus, pre-testing is conducted to assess the spatial preference of each group of mice, with one compartment was black with a stainless steel grid rod floor, and another compartment was white a with grid fastened floor. And then, LY-2183240 was administered via intraperitoneal (i.p.) injection every other day and placed in the non-preference chamber, whereas saline was injected i.p. when placing the mice in the preference chamber (Figure 7A). Mice injected with 1 mg/kg of LY-2183240 showed a decrease in time in preference place (s) and an increase in time in the non-preference place. In contrast, the group of mice injected with saline did not exhibit significant differences (Figures 7B and 7C). However, according to the CPP score calculation, no significant differences were observed between the two groups, indicating that CPP induced by LY-2183240 were not elicited (Figure 7D). Nevertheless, LY-2183240 alters place preferences (repeated measures ANOVA $F(3,30) = 6.618$, interaction between places and tests **$p = 0.0015$). We investigated *in vivo* cell death effect of LY-2183240 in CPP experiment to prove a small portion of cell death derived from *in vitro* results (Figures 4 and 5). The number of DAPI+ cells was reduced in dentate gyrus (DG) of hippocampus (Figures 7E and 7F) and cortex (Figures 7E and 7H). The number of NeuN+ cells was reduced in CA3 and CA1 of hippocampus (Figures 7E and 7G). These results are consistent with the results of *in vitro* cell death.

DISCUSSION

In this study, we attempted to evaluate the effects of LY-2183240 as a drug on the CNS. We observed an increase in the number of APs from both mouse primary cortical neurons and hippocampal CA1 pyramidal neurons. Enhancing the RMP triggers an increase in sAPs, subsequently leading to the release of more glutamate. This elevated concentration of glutamate in the extracellular region can result in glutamate excitotoxicity, ultimately leading to neuronal cell death. Remarkably, LY-2183240 has been found to enhance the bar pressing score in SA tests and alter both preference and non-preference dwelling times in CPP tests. These findings suggest that LY-2183240 induces reinforcement in

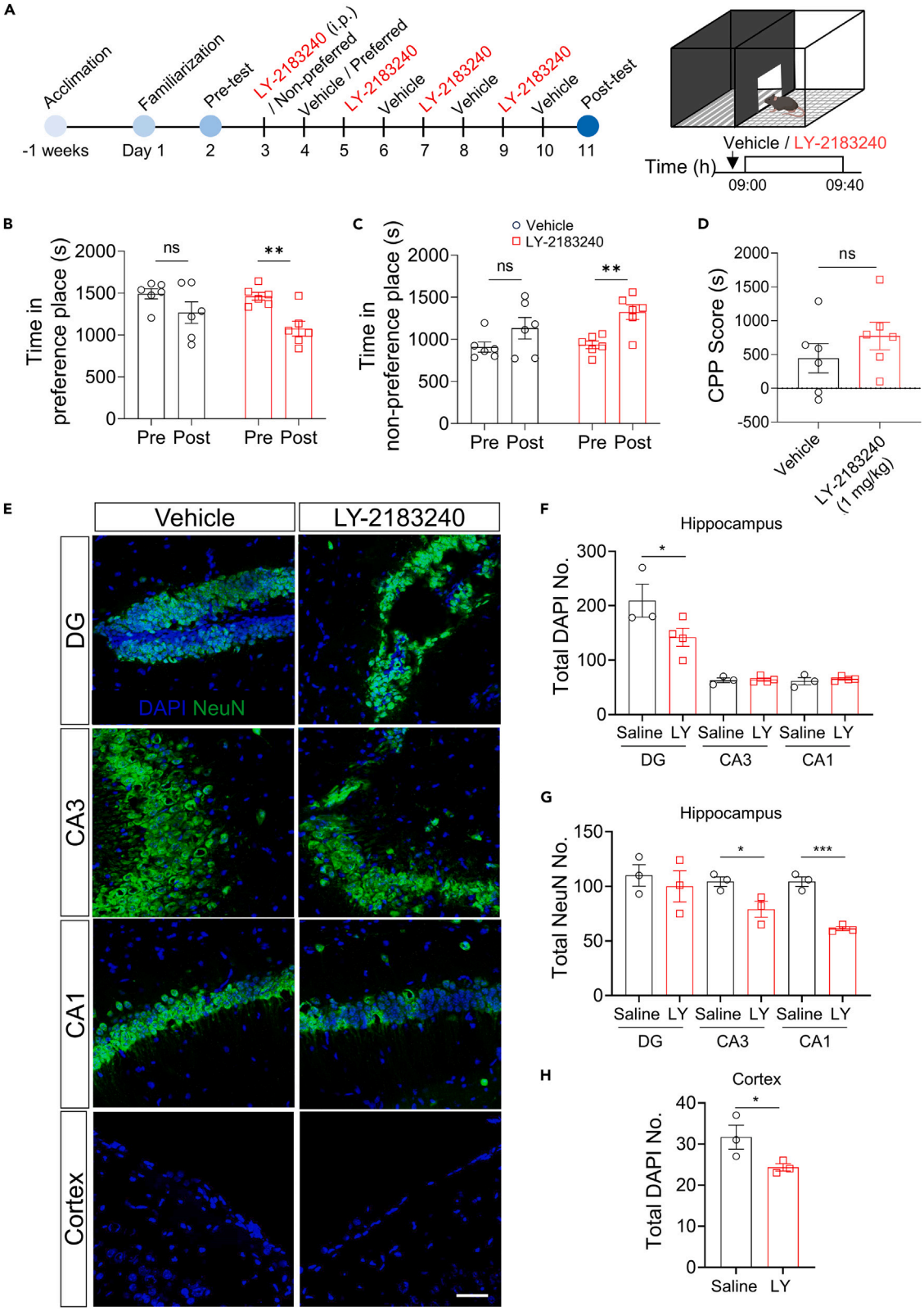
A
Acclimation
Familiarization
Pre-test
LY-2183240 (i.p.)
/ Non-preferred
Vehicle / Preferred
LY-2183240
Vehicle
LY-2183240
Vehicle
LY-2183240
Vehicle
Post-test
-1 weeks
Day 1
2
3
4
5
6
7
8
9
10
11
Vehicle / LY-2183240
Time (h)
09:00
09:40
B
Time in preference place (s)
ns
**
Pre Post
Pre Post
C
Vehicle
LY-2183240
Time in non-preference place (s)
ns
**
Pre Post
Pre Post
D
CPP Score (s)
ns
Vehicle
LY-2183240 (1 mg/kg)
E
Vehicle
LY-2183240
DG
CA3
CA1
Cortex
DAPI NeuN
F
Hippocampus
Total DAPI No.
*
Saline LY Saline LY Saline LY
DG
CA3
CA1
G
Hippocampus
Total NeuN No.
*
***
Saline LY Saline LY Saline LY
DG
CA3
CA1
H
Cortex
Total DAPI No.
*
Saline LY

Figure 7. Four times intraperitoneal (i.p.) injections of 1 mg/kg LY-2183240 do not significantly reduce the score of conditioned place preference (CPP), but do show the change of individual component by both the reduction of preference place and the increase of non-preference place

(A) Timeline for LY-2183240 CPP procedure (left). Each group of mice underwent preference tests for 30 min each (right). i.p. injection group: saline and LY-2183240 (1 mg/kg).

(B and C) Summarized bar graph of time in (B), preference place(s) (unpaired t test. ns, p value = 0.15 and $^{**}p < 0.01$, $n = 6$) and (C), non-preference place(s) (unpaired t test, ns, $p = 0.15$ and $^{**}p < 0.01$, $n = 6$) with saline and LY-2183240. Two-way ANOVA: tests F(1,40) = 4.152e-010, $p > 0.99$; places F(3,40) = 6.574, $p = 0.001$; interaction between tests and places F(3,40) = 8.824, $p = 0.00001$, $n = 6$.

(D) Summarized bar graph of CPP score(s) with saline and LY-2183240 (unpaired t test. ns, $n = 6$).

(E) Representative fluorescent images of hippocampal DA, CA3, CA1, and cortex from the mouse brain after CPP experiment. Nuclei were stained with DAPI (blue). Neuronal nuclei were stained with NeuN (green). Vehicle control (left) and LY-2183240 (right). Scale bar: 50 μm.

(F–H) Bar graphs summarizing the number of (F) total DAPI (unpaired t test, ns, $p = 0.0447$ and $^{*}p < 0.05$, $n = 3$–4), (G) NeuN (unpaired t test, n.s., $^{*}p = 0.021$ and $^{***}p = 0.0004$, $n = 4$) in hippocampus, and (H) total DAPI in cortex (unpaired t test, p value = 0.0366 and $^{*}p < 0.05$, $n = 3$). Data are represented as mean ± SEM.

CPP behavior. Our findings suggest that LY-2183240 exhibits reinforcing properties that may indicate some potential for abuse. However, further *in vivo* and behavioral investigations are necessary to more conclusively determine its addictive potential. This effect is proposed to occur through a mechanism involving the increased excitability and subsequent death of approximately 15% of specific population of neurons.

Almost 50 years ago, glutamate excitotoxicity emerged as a cell death mechanism initiated by the excessive release of glutamate from both neurons and glial cells.[26] Excitotoxicity is common in various chronic disorders of the CNS and is regarded as the primary mechanism underlying both neuronal dysfunction and cell death in acute CNS diseases. Excitotoxic cell damage can result from various mechanisms and pathways, incorporating pro-death signaling cascades downstream of glutamate receptors, Ca^{2+} overload, oxidative stress, mitochondrial dysfunction, elevated glutamate levels in the synaptic cleft, and disrupted energy metabolism.[27] In our experimental conditions, the incubation of 100 μM LY-2183240 resulted in approximately a 5-fold increase in extracellular glutamate concentration compared to the control (Figure 3D). After a 20 h incubation with 100 μM LY-2183240, the glutamate concentration in the extracellular region rises by over 6 mM, potentially triggering cell excitotoxicity. The pro-apoptotic cell death caused by LY-2183240-mediated excitotoxicity does probably lead to the death of GABAergic interneurons, causing disinhibition.

When assessing the potency of drugs with unclear mechanisms, it's crucial to initially determine the optimal dosage by considering factors such as cytotoxicity and the mode of action associated with a particular dose. In fact, 0.05 mg/kg of LY-2183240 was utilized to compare with 0.01 mg/kg of methamphetamine in the SA study. This dosage of 0.05 mg/kg can be converted to 0.16 μM LY-2183240, while 0.01 mg/kg of methamphetamine equates to 0.07 μM, a well-established reference drug dosage. As observed in our experiments, 7.8 μg of LY-2183240, estimated to be equivalent to 13 infusion number for 12 days from a concentration of 0.05 mg/mL, resulted in neuronal death (Figures 4 and 5), reduced arborization (Figure 4), an increase in glutamate release (Figure 3), and neuronal apoptosis at a concentration of 10 μM *in vitro*. Hence, we propose that the appropriate *in vivo* dose can be determined based on the effective *in vitro* mode of action at the initially estimated dose.

Various psychoactive drugs, such as methamphetamine, cocaine, morphine, and nicotine, induce neurotoxicity, leading to neuronal cell death.[28–31] Multiple studies have indicated that neuronal death induced by methamphetamine is closely associated with programmed cell death signaling pathways, including apoptosis, necroptosis, pyroptosis, and ferroptosis.[32,33] Prolonged use of morphine can lead to neuronal apoptosis in the brain by upregulating the expressions of pro-apoptotic proteins such as Fas and caspase-3, while simultaneously downregulating the expression of the anti-apoptotic protein Bcl-2.[31] Cocaine treatment caused cell death via apoptosis and necrosis, as indicated by mitochondrial dysfunction, elevated lactate dehydrogenase (LDH) release, caspase 3 activation, decreased Bcl-2 expression, and increased α-spectrin cleavage.[29] Similar to widely recognized addictive substances, our findings demonstrate that LY-2183240 also induces neuronal cell death and potentially acting as a reinforcer (albeit weaker than methamphetamine).

Endocannabinoid signaling commonly regulates a synaptic plasticity mechanism where a postsynaptic cell retrogradely modulates the reduction of vesicle release from presynaptic terminals that make contact with it. LY-2183240 can accumulate endogenously released endocannabinoids in the extracellular region by blocking the endocannabinoid transporter, thus reducing presynaptic neurotransmitter release through the activation of presynaptic CB1 receptors. LY-2183240 was identified as a potent inhibitor of FAAH, with an IC_{50} of 12 nM. However, in our study, we observed that concentrations ranging from 10 to 100 μM of LY-2183240 increased neuronal excitability instead of reducing synaptic transmission. This suggests a distinct physiological function of LY-2183240 at higher concentrations in the brain.

Limitations of the study

Our findings suggest that LY-2183240 acts as a reinforcer, but there is insufficient scientific evidence to conclude that it is addictive. Therefore, further experiments are necessary to support this conclusion.

We explain the mechanism by which LY-2183240-induced neuronal excitability leads to apoptosis as likely being due to the death of certain neuron types. However, this paper acknowledges that the research on the related mechanisms is insufficient. Thus, additional studies are necessary to provide robust scientific evidence for the susceptibility of the certain type of inhibitory neurons on the effect of LY-2183240.

RESOURCE AVAILABILITY

Lead contact

Requests for further information and resources should be directed to the lead contact, Dong Ho Woo (dongho.woo@kitox.re.kr).

Materials availability

This study did not generate new unique reagents.

Data and code availability

- The lead contact will share all data reported in this paper upon request.
- This paper dose not report original code.
- Any additional information required to reanalyze the data reported in this paper is available from the lead contact upon request.

ACKNOWLEDGMENTS

This work is supported by the Intramural Research Program (1711195891) of the Korea Institute of Toxicology (KIT, KK-2313), by the National Research Council of Science & Technology grant by the Korea government (MSIT) (No. GTL24021-400), and by a grant 23212MFDS216 (1475014003, IP-2305 to D.H.W.) from the Ministry of Food and Drug Safety in 2023.

AUTHOR CONTRIBUTIONS

K.-S.H and D.H.W. supervised the study and wrote the manuscript. Y.Y.J. performed all rat primary cell cultures and various *in vitro* experiments including imaging, cell viability, immunocytochemistry, and CPP. J.H.Y. performed whole patch clamp for measuring AP *in vitro* and *ex vivo* and conducted glutamate assay. S.Y.J. preformed flow cytometry. S.J.P., N.Y.L., and S.W.S. conducted SA.

DECLARATION OF INTERESTS

The authors declare no competing interests.

STAR★METHODS

Detailed methods are provided in the online version of this paper and include the following:

Received: April 29, 2024
Revised: July 29, 2024
Accepted: September 26, 2024
Published: September 30, 2024

REFERENCES

1. Mechoulam, R., and Parker, L.A. (2013). The endocannabinoid system and the brain. Annu. Rev. Psychol. *64*, 21–47.
2. Devane, W.A., Hanus, L., Breuer, A., Pertwee, R.G., Stevenson, L.A., Griffin, G., Gibson, D., Mandelbaum, A., Etinger, A., and Mechoulam, R. (1992). Isolation and structure of a brain constituent that binds to the cannabinoid receptor. Science *258*, 1946–1949.
3. Di Marzo, V., Bifulco, M., and De Petrocellis, L. (2004). The endocannabinoid system and its therapeutic exploitation. Nat. Rev. Drug Discov. *3*, 771–784.
4. Pertwee, R.G. (2008). The therapeutic potential of drugs that target cannabinoid receptors or modulate the tissue levels or actions of endocannabinoids. Drug Addic. Basic Res. Ther. *1*, 637–686.
5. Janero, D.R., Vadivel, S.K., and Makriyannis, A. (2009). Pharmacotherapeutic modulation of the endocannabinoid signalling system in psychiatric disorders: drug-discovery strategies. Int. Rev. Psychiatry *21*, 122–133.
6. Dickason-Chesterfield, A.K., Kidd, S.R., Moore, S.A., Schaus, J.M., Liu, B., Nomikos, G.G., and Felder, C.C. (2006). Pharmacological characterization of endocannabinoid transport and fatty acid amide hydrolase inhibitors. Cell. Mol. Neurobiol. *26*, 407–423.
7. Moore, S.A., Nomikos, G.G., Dickason-Chesterfield, A.K., Schober, D.A., Schaus, J.M., Ying, B.-P., Xu, Y.-C., Phebus, L., Simmons, R.M.A., Li, D., et al. (2005). Identification of a high-affinity binding site involved in the transport of endocannabinoids. Proc. Natl. Acad. Sci. USA *102*, 17852–17857.
8. Powers, M.S., Barrenha, G.D., Mlinac, N.S., Barker, E.L., and Chester, J.A. (2010). Effects of the novel endocannabinoid uptake

inhibitor, LY2183240, on fear-potentiated startle and alcohol-seeking behaviors in mice selectively bred for high alcohol preference. Psychopharmacology (Berl) *212*, 571–583. https://doi.org/10.1007/s00213-010-1997-2.

9. Tutka, P., Wlaź, A., Florek-Łuszczki, M., Kołodziejczyk, P., Bartusik-Aebisher, D., and Łuszczki, J.J. (2018). Arvanil, olvanil, AM 1172 and LY 2183240 (various cannabinoid CB1 receptor agonists) increase the threshold for maximal electroshock-induced seizures in mice. Pharmacol. Rep. *70*, 106–109.
10. Deutsch, D.G., and Chin, S.A. (1993). Enzymatic synthesis and degradation of anandamide, a cannabinoid receptor agonist. Biochem. Pharmacol. *46*, 791–796.
11. Alexander, J.P., and Cravatt, B.F. (2006). The putative endocannabinoid transport blocker LY2183240 is a potent inhibitor of FAAH and several other brain serine hydrolases. J. Am. Chem. Soc. *128*, 9699–9704.
12. Oh, H.-A., Lee, J.-H., and Woo, D.H. (2022). Acute effects of 4-EA-NBOMe, 3, 4-DCMP, LY-2183240 and AB-CHFUPYCA on the excitability of rat cortical primary cultured neurons. Mol. Cell. Toxicol. *18*, 531–538.
13. Uchiyama, N., Matsuda, S., Kawamura, M., Shimokawa, Y., Kikura-Hanajiri, R., Aritake, K., Urade, Y., and Goda, Y. (2014). Characterization of four new designer drugs, 5-chloro-NNEI, NNEI indazole analog, α-PHPP and α-POP, with 11 newly distributed designer drugs in illegal products. Forensic Sci. Int. *243*, 1–13.
14. Sedefov, R., Gallegos, A., Mounteney, J., and Kenny, P. (2013). Monitoring Novel Psychoactive Substances: A Global Perspective. In Novel Psychoactive Substances (Elsevier), pp. 29–54.
15. Evans-Brown, M., Gallegos, A., Francis, W., Christie, R., Cunningham, A., Sekula, J., Almeida, A., and Sedefov, R. (2015). European Monitoring Centre for Drugs and Drug Addiction (Luxembourg: European Union Publications Office).
16. De Coning, E., and Stølsvik, G. (2013). United Nations Office on Drugs and Crime. Int. J. Mar. Coast. Law *28*, 189–204.
17. King, L., and Kicman, A. (2011). A Brief History of 'new Psychoactive Substances (Wiley Online Library).
18. Madras, B.K. (2017). The growing problem of new psychoactive substances (NPS). Curr. Top. Behav. Neurosci. *32*, 1–18.
19. Shafi, A., Berry, A.J., Sumnall, H., Wood, D.M., and Tracy, D.K. (2020). New psychoactive substances: a review and updates. Ther. Adv. Psychopharmacol. *10*, 2045125320967197.
20. Pantano, F., Graziano, S., Pacifici, R., Busardò, F.P., and Pichini, S. (2019). New psychoactive substances: a matter of time. Curr. Neuropharmacol. *17*, 818–822.
21. Robins, M.T., Blaine, A.T., Ha, J.E., Brewster, A.L., and Van Rijn, R.M. (2019). Repeated use of the psychoactive substance ethylphenidate impacts neurochemistry and reward learning in adolescent male and female mice. Front. Neurosci. *13*, 124.
22. Miliano, C., Serpelloni, G., Rimondo, C., Mereu, M., Marti, M., and De Luca, M.A. (2016). Neuropharmacology of new psychoactive substances (NPS): focus on the rewarding and reinforcing properties of cannabimimetics and amphetamine-like stimulants. Front. Neurosci. *10*, 153.
23. Oh, H.-A., Yoo, J.H., Kim, Y.-J., Han, K.-S., and Woo, D.H. (2023). 4-EA-NBOMe, an amphetamine derivative, alters glutamatergic synaptic transmission through 5-HT1A receptors on cortical neurons from SprageDawley rat and pyramidal neurons from C57BL/6 mouse. Neurotoxicology *95*, 144–154.
24. Thomsen, M., and Caine, S.B. (2007). Intravenous drug self-administration in mice: practical considerations. Behav. Genet. *37*, 101–118.
25. Huston, J.P., Silva, M.A.d.S., Müller, C.P., and Müller, C.P. (2013). What's conditioned in conditioned place preference? Trends Pharmacol. Sci. *34*, 162–166.
26. Olney, J.W. (1971). Glutamate-induced neuronal necrosis in the infant mouse hypothalamus: an electron microscopic study. J. Neuropathol. Exp. Neurol. *30*, 75–90.
27. Neves, D., Salazar, I.L., Almeida, R.D., and Silva, R.M. (2023). Molecular mechanisms of ischemia and glutamate excitotoxicity. Life Sci. *328*, 121814.
28. Guo, D., Huang, X., Xiong, T., Wang, X., Zhang, J., Wang, Y., and Liang, J. (2022). Molecular mechanisms of programmed cell death in methamphetamine-induced neuronal damage. Front. Pharmacol. *13*, 980340.
29. Lepsch, L.B., Munhoz, C.D., Kawamoto, E.M., Yshii, L.M., Lima, L.S., Curi-Boaventura, M.F., Salgado, T.M.L., Curi, R., Planeta, C.S., and Scavone, C. (2009). Cocaine induces cell death and activates the transcription nuclear factor kappa-B in PC12 cells. Mol. Brain *2*, 3–15.
30. Berger, F., Gage, F.H., and Vijayaraghavan, S. (1998). Nicotinic receptor-induced apoptotic cell death of hippocampal progenitor cells. J. Neurosci. *18*, 6871–6881.
31. Liu, L.-W., Lu, J., Wang, X.-H., Fu, S.-K., Li, Q., and Lin, F.-Q. (2013). Neuronal apoptosis in morphine addiction and its molecular mechanism. Int. J. Clin. Exp. Med. *6*, 540–545.
32. Huang, E., Huang, H., Guan, T., Liu, C., Qu, D., Xu, Y., Yang, J., Yan, L., Xiong, Y., Liang, T., et al. (2019). Involvement of C/EBPβ-related signaling pathway in methamphetamine-induced neuronal autophagy and apoptosis. Toxicol. Lett. *312*, 11–21.
33. Wen, D., Hui, R., Wang, J., Shen, X., Xie, B., Gong, M., Yu, F., Cong, B., and Ma, C. (2019). Effects of molecular hydrogen on methamphetamine-induced neurotoxicity and spatial memory impairment. Front. Pharmacol. *10*, 823.

STAR★METHODS

KEY RESOURCES TABLE

REAGENT or RESOURCE	SOURCE	IDENTIFIER
Drugs		
LY-2183240	Korea Food and Drug Administration	N/A
Methamphetamine	Korea Food and Drug Administration	N/A
delta-p tetrahydrocannabinol (THC)	Korea Food and Drug Administration	N/A
Experimental models: Organisms/strains		
C57BL/6N male mice	Orientbio	N/A
C57BL/6 female mouse embryonic	Koatech	N/A
C57/BL6J male mice	Orientbio	N/A
Critical commercial assays		
Cell counting kit-8 (CCK-8)	Dojindo laboratories	CK-04
Glutamate assay kit	Abcam	ab83389
FITC Annexin V Apoptosis Detection Kit I	BD Biosciences	556547 RRID:AB_2869082
Antibodies and staining resources		
FITC Annexin V	BD biosciences	#51-65874X
Anti-MAP2 antibody	abcam	ab32454, RRID:AB_776174
Anti-NeuN antibody	Millipore	ABN90, RRID:AB_11205592
Chemicals, peptides, and recombinant proteins		
AM6545	Biotechne	5443
Softwares		
Mini analysis	Synaptosoft	Mini Analysis Program; RRID: SCR_002184
Clampfit	Molecular Devices	pClamp; RRID: SCR_011323
GraphPad Prism	GraphPad software	GraphPad Prism; RRID: SCR_002798
Activity Monitor 5.0 software	Med Associates	Activity Monitor 5.0 software
ImageJ	National Institutes of Health	ImageJ; RRID: SCR_003070
Confocal software	Olympus	FV30S-SW

EXPERIMENTAL AND MODEL AND STUDY PARTICIPANT DETAILS

Animals

Primary cultured neurons were obtained from C57BL/6 female mouse embryos at embryonic day 16 (Koatech, Korea). Brain slices were prepared from three-week-old male C57BL/6 mice (OrientBio, Korea). Animals for the experiments (locomotor activity test, SA, CPP) were obtained at 6 weeks-old male C57BL/6 mice and were used at 7 weeks of age at the start of injection. All experiments were conducted in accordance with animal study protocols approved by the Institutional Animal Care and Use Committee of the Korea Institute of Toxicology (IAC-24-01-0028, IAC-23-01-0382 and IAC-23-01-0383, KIT, Daejeon, Korea) and Ministry of Food and Drug Safety (MFDS-20-021, Cheongju, Korea). Animal care was performed following National Institutes of Health (NIH) guidelines. IAC-24-01-0028, IAC-23-01-0382, IAC-23-01-0383, and MFDS-20-021.

Chemicals

LY-2183240 and methamphetamine was obtained from the Korea Food and Drug Administration. The stock concentration of LY-2183240 was 100 mM with a final working concentration was 10 μM. 0.05 mg/kg LY-2183240 for *in vivo* experiment is equivalent to 162 nM in *in vitro* experiment. Because 100 μM LY-2183240 is too cytotoxic, *in vitro* mechanistic studies were conducted with 10 μM in majority. 0.1 mg/kg methamphetamine was used for SA.

METHOD DETAILS

Culturing mouse cortical neurons

Primary neurons were cultured from E15 ~ E16 C57BL/6 embryos. After dissection of the cortex with forceps, the tissue was placed in cold Hanks's balanced Salt Solution (WELGENE, LB 003–04). The cells were dissociated using 0.25% trypsin-EDTA (Gibco, 25200056) for 10 min at 37°C. Trypsin was inactivated by adding DMEM containing 10% FBS. The media was decanted and replaced with Neurobasal media (Gibco, MA, USA) containing 2% B-27 supplement (Gibco, MA, USA), 1% L-glutamine (2 mM, Gibco, MA, USA) and 1% penicillin-streptomycin. The cell suspension was passed through a fire-polished Pasteur pipette rigorously and was repeated 2–3 times. Cells were then passed through a cell strainer with a pore size of 100 μm (SPL, Seoul, Korea) and 40 μm (SPL, Seoul, Korea) to remove non-triturated tissue. Cells were plated at 1.2×10^5 per mL of a 24-well plate onto surfaces coated with 50 μg/mL of Poly-D-lysine (PDL) (Sigma, P1024). A half media change was conducted every 48 h. Cultures were maintained in a humidified atmosphere containing 5% CO_2 and 95% O_2 at 37°C for 12–16 days.

Cell counting kit-8 (CCK-8) assay

To assess the effect of LY-2183240 on cell viability, CCK-8 (Promega, WI, USA) was used. Neurons were seeded on the 96-well plate (8×10^4 neurons/well) and treated with 0.001, 0.01, 0.1, 1, 10, 50, 100 μM LY-2183240 and blank for 24 h. Dye solution was added for 2 h in a 5% CO_2/95% O_2 incubator at 37°C. Absorbance was measured at 450 nm using a microplate reader (GloMax explorer multimode, Promega, WI, USA).

Electrophysiology from primary culture neurons

Whole-cell patch clamp recordings were conducted on cultured cortical neurons using a Multiclamp 700B amplifier and Digidata 1550B system (Molecular Devices). The recording chamber was filled with an external solution containing (in mM) 150 NaCl, 3 KCl, 10 HEPES, 22 Sucrose, 5.5 Glucose, 2 $MgCl_2$, 2 $CaCl_2$ (pH 7.4). Recording pipettes (4–7 MΩ resistance) were filled with an internal solution for sEPSP recordings composed of (in mM) 130 KCl, 5 NaCl, 10 HEPES, 0.4 $CaCl_2$, 10 EGTA (pH 7.3). Current injection-induced APs were recorded using an internal solution containing (in mM) 126 K-gluconate, 10 HEPES, 0.5 $MgCl_2$, 10 BAPTA (pH 7.2). For mEPSC recordings, an internal solution with (in mM) 135 Cs-methanesulfonate, 0.2 EGTA, 10 HEPES, 10 KCl, 1 MgCl (pH 7.3) was used in combination with an external solution containing 1 μM TTX. All electrophysiology data from cultured cells were analyzed using Clampex 10 (Molecular Devices), Clampfit (Molecular Devices) and Mini analysis (Synaptosoft).

Brain slice preparation

C57BL/6 Male mice (3 weeks) were deeply anesthetized with 2,2,2,-Tribromoethanol (Sigma, T48402) in 0.9% saline. Horizontal sections were performed in ice-cold artificial cerebrospinal fluid (ACSF) containing (in mM) 130 NaCl, 24 $NaHCO_3$, 3.5 KCl, 1.25 NaH_2PO_4, 1 $CaCl_2$, 2 $MgCl_2$, 10 Glucose (pH 7.4), saturated with 95% O_2 and 5% CO_2. The sections were sliced with 300 μm thickness using vibrating microtome (Leica, VT1000S), and stored at room temperature (RT) in an incubation chamber with ACSF for 1 h for slice stabilization prior to recording.

Electrophysiology from mouse brain slices

Whole-cell patch-clamp recordings of mouse hippocampal slices under voltage clamp (holding potential −70 mV) were performed with a MultiClamp 700B amplifier and digitized with a Digidata 1322A data acquisition system (Molecular Devices, CA, USA). Mouse hippocampal slices were transferred to a recording chamber with ACSF, which was saturated with 95% O_2 and 5% CO_2. The ACSF solution was composed of (in mM) 130 NaCl, 1.25 NaH2PO_4, 3.5 KCl, 24 $NaHCO_3$, 1.5 $CaCl_2$, 1.5 $MgCl_2$ and 10 glucose. Borosilicate glass capillaries (cat. no. 1B150F-4, outer diameter, 1.50 mm; inner diameter, 1 mm; World Precision Instruments, FL, USA) with a tip resistance of 3~8 MΩ were pulled (P-97 micropipette puller, Sutter Instrument, Novato, CA, USA). Glass capillaries for AP (AP) recordings were filled with an intracellular solution consisting of (in mM) 140 K-gluconate, 10 HEPES, 7 NaCl, 4 Mg-ATP, and 0.3 Na-GTP (pH adjusted to 7.4 with KOH; osmolarity adjusted to 280–290 mOsm/L). Each patched cell was inspected in current clamp mode, and neurons were subjected to 10 depolarizing current pulses in 20 pA increments for 0.5 s each at 2 s intervals. The membrane potentials, initially adjusted to −60 mV, were returned to the resting potential. Glass capillaries for excitatory postsynaptic current recording were filled with (in mM) 150 CsMeSO4, 10 NaCl, 0.5 CaCl2, 10 HEPES (pH adjusted to 7.3 with CsOH; osmolality adjusted to 300 mOsmol/kg with sucrose), and 2–5 mM QX 314. All electrophysiology data from slices were analyzed using Clampex 10 (Molecular Devices) and Clampfit (Molecular Devices).

Calcium imaging

The external solution contained (mM): 150 NaCl, 10 HEPES, 3 KCl, 2 $CaCl_2$, 2 $MgCl_2$ and 5.5 glucose (pH adjusted to pH 7.3–7.4). Intensity images at a wavelength of 510 nm were acquired from excitation wavelengths of 340 and 380 nm using Electron Multiplying Charge-Coupled Device camera (Ixon 867, Andor Oxford instrument). Neurons were incubated for 40 min with 5 μM fura-2 a.m. (Thermofisher, MA, USA) and 5 μL pluronic F-127 (Thermofisher, MA, USA). 100 μM glutamate, 50 μM glycine and 10 μM LY-2183240 were applied for 30-50 s to stimulate Ca^{2+} transients. Images are acquired every 1 s. In the field of view, 50 cells were measured and analyzed.

Glutamate concentration assay

All reagent included in the glutamate assay kit (Abcam, ab83389) were stored at −20°C after aliquoting, and all procedures were executed according to the protocol supplied by abcam (https://www.abcam.com/en-kr/products/assay-kits/glutamate-assay-kit-ab83389). The medium, standardized to a volume of 1 mL, was harvested, and the supernatant was collected and centrifuged at 13,000 rpm for 1 min to remove cell debris. We reproduced 0, 2, 4, 6, 8, and 10 nM using the provided 0.1M glutamate standard. A 1/10 and 1/20 dilution of the harvested medium was performed using assay buffer. We added these samples and 100 μL of reaction mix (90 μL assay buffer, 8 μL developer, and 2 μL enzyme) to each well simultaneously. The sample was protected from light and reacted for 30 min at 37°C. The absorbance was measured at 450 nm, and the concentration was calculated according to the following formula.

$GlutamateConcentration = \left(\frac{S_a}{S_v}\right) \times D$. ($S_a$ = Amount of sample (nmol) from the standard curve, S_v = Volume of sample (μL) added into the well, D = Sample dilution factor).

Immuncytochemistry (ICC) of mouse cultured neurons

Cultured neurons on the coverslip were fixed for 15 min in 4% paraformaldehyde (PFA). Neurons were washed with Phosphate-Buffered Saline (PBS) 3 times and incubated with a blocking solution for 1 h (0.5% Triton X-100, 1% BSA, 5% normal goat serum in PBS) at RT. Primary antibodies in the blocking solution were incubated overnight at 4°C. Primary antibodies were diluted to the following amounts: anti-NeuN antibody (Abcam, CB, UK) 1:1000 and anti-MAP2 antibody (Abcam, CB, UK) 1:1000. After washing with PBSTB (0.5% Triton X-100, 1% BSA in PBS) twice for 10 min each, cells were incubated with secondary antibodies in PBSTB for 1 h at RT. Secondary antibodies were diluted to the following amounts: Alexa Fluor 488 goat anti-mouse and Alexa Fluor 594 goat anti-rabbit 1:1000. After washing with PBST for 10 min twice and PBS for 10 min once at RT, neurons on coverslips were incubated with a mounting medium including DAPI (VECTASHIELD, CA, USA) and mounted onto a slide glass. A series of fluorescent images were obtained by confocal microscope (Olympus, Tokyo, Japan) and analyzed by ImageJ software.

Immunohistochemistry (IHC) of mouse brain

Mice were anesthetized using 2% avertin and perfused with 0.1M PBS, followed by 4% paraformaldehyde (PFA). Brains were post-fixed in 4% PFA at 4°C for 24 h and then 30% sucrose 4°C for 48 h. Brains were cut in coronal sections of 16 mm on a cryosection. Sections were washed two times in 1× PBS without calcium chloride and magnesium and then were blocked in 1× PBS containing 5% NGS, 2% BSA and 0.5% Triton X-100 (blocking solution). Primary antibody used are as follow: Guinea pig anti-NeuN (1:2000, ABN90, Millipore), The brain samples with primary antibodies were incubated overnight at 4°C. Then, the sections were washed three times in 1× PBS containing 0.5% BSA and 0.5% Triton X-100 (PBSTB) and incubated in proper secondary antibodies from the invitrogen for 1 h in RT. After three rinses in 1× PBS containing 0.5% Triton X-100 (PBST) and DAPI staining at antifade mounting medium with DAPI (VECTASHIELD), the sections were mounted on polysine microscopic slide glass (Thermo Scientific). Brain images were acquired using a Olympus FV3000 confocal microscope.

Flow cytometry

Cells were plated at 1.2 × 10^5 cells/mL density in 24-well plates and treated with LY2183240. The cells were rinsed in PBS and resuspended in 1× Binding Buffer (#556547, BD, USA) at 1.2 × 10^5 cells/mL concentration. Annexin V and PI staining were used to separate healthy, early-apoptotic, late-apoptotic, and necrotic cells by flow cytometric analysis. After transferring 100 μL of the solution (1 × 10^5 cells) into a new tube, mix with 5 μL of annexin V (#556547, BD, USA) and 5 μl of propidium iodide. Incubate for 15 min at RT in the dark. Following incubation, add 1× Binding Buffer to each tube until the liquid volume reaches 500 μL. CytoFLEX S (Beckman Coulter, USA) was used to determine the amount of apoptotic cells.

Locomotor activity test

The locomotor activity test was performed in a square acrylic container (43 cm × 43 cm x 31 cm, length x width x height), with an open field with infrared beam sensors at the bottom (ENV-520; Med Associates, Inc., St. Albans, VT, USA). For the first 3 days, mice (n = 8 per group) were habituated for 60 min in an open field apparatus to minimize the effects of environmental changes. On the test day (day 4), mice were treated with LY-2183240 (0.1, 0.25, 5, 1, and 3 mg/kg, i.p.) and allowed to move freely for 60 min. Distance traveled served as a measure of locomotor activity. As a positive control group, METH (1 mg/kg, i.p.) was injected to verify the measurement of locomotor activity. Thereafter, mice movement distance (cm) and movement time (sec) were recorded using Activity Monitor 5.0 software (SOF-812; Med Associates, Inc., St. Albans, VT, USA).

Self-administration

The apparatus for SA training and testing consisted of one chamber polyvinyl chloride (PVC) boxes. The SA apparatus (MED-307A-CT-B1) was purchased from Med Associates Inc. (St. Albans, VT, USA). The SA test uses an operant conditioning chamber (43 × 43 × 31 cm (W × D ×H)) within a sound- and light-attenuating cubicle box. The chamber is equipped with two response levers (active and inactive lever), house light, cue light, and an infusion pump. A computerized system (Med-PC) connected to SA test equipment was used for data recording. Prior to food training, food was restricted to facilitate the spontaneous lever-pressing response training of the mice (limited to 3 g mouse for each day). During the three days of food training, mice were trained to acquire food pellets (20 mg, Dustless Precision Pellets Rodent, Bio-Serv.,

Frenchtown, NJ, USA) according to a fixed rate 1 reinforcement schedule. On the first day, it was performed overnight, and on the other two days, it was conducted for 3 h. As a food training acquisition criterion, only mice that acquired more than 90 food pellets for three consecutive days were selected (A maximum of 100 food pellets per mouse allowed). The mouse's dorsal catheter port is connected to the syringe and the auto infusion pump. For catheter implantation surgery, animals were anesthetized with pentobarbital sodium (50 mg/kg; Entobar, Hanlim Pharmaceuticals, SEOUL, Korea), and a catheter (26-gauge, 0.3 mm inner diameter, 0.64 mm outer diameter; Plastic One, Roanoke, VA, USA) was inserted into the right jugular vein of each mouse. The catheters were flushed with 0.2 mL of the antibiotic gentamicin sulfate (0.32 mg/mL; Shin Poong Pharm Co., Ltd., Seoul, Korea) in heparinized saline (30 IU/mL; JW-Pharma Co., Ltd., Seoul, Korea) every day during the experimental period. During the SA test period, heparin is administered intravenously a total of 2 times (once before experiment and once after).

After a recovery period of at least 7 days, mice were allowed to self-administer (i.v.) vehicle (DMSO:tween80:saline = 1:1:8; v/v), LY-2183240 (0.05 mg/kg/infusion), and methamphetamine (0.1 mg/kg/infusion) for 2 h per day for 12 days. A single press of the lever delivered a 10 μL drug solution for 5-s and activated the cue light simultaneously. A 20-s timeout period then followed, during which both the house light and cue light were turned off and no drug was delivered.

Conditioned place preference

The apparatus for CPP training and testing consisted of two compartments polyvinyl chloride (PVC) boxes. One compartment (20 cm long, 20 cm wide, and 30 cm high) was black with a stainless-steel grid rod floor, and another compartment was white a with grid fastened floor. Two compartments are divided by wall which has a door. After finishing CPP experiments, the analysis of behavior was conducted in a blind manner.

Pre-conditioning (Days 1, 2)

During the preconditioning phase of the experiment, the door between two compartments was open. Mice moved around two compartments for habituation for 40 min on day 1. The time spent in each of the compartments was recorded for 40 min on day 2 to determine preferred or non-preferred compartment.

Conditioning (Days 3–10)

For the CPP experiment with LY-2183240 i.p. (Intraperitoneal) injection, we administered 1 mg/kg just before placing the mice into non-preferred compartment of CPP chamber on days 3, 5, 7 and 9. On days 4, 6, 8 and 10, Vehicle group (DMSO:tween-80:saline = 1:1:8; v/v) was administered into intraperitoneal in the same way to LY-2183240 and the mice were placed into preferred compartment.

Post-conditioning test (Day 11)

With the chamber door open, the mouse movement was recorded for a total of 40 min. The preference score was calculated for each animal as follow: Preference score = (preferred – non-preferred) before + (non-preferred – preferred) after.

QUANTIFICATION AND STATISTICAL ANALYSIS

ICC and IHC analysis

Confocal microscopic images were analyzed using the ImageJ program (NIH).

Statistical analysis

GraphPad Prism 9.1.2 (GraphPad Software) was used for data presentation and statistical analysis. The variance of two samples groups were analyzed with the one-tailed or two-tailed unpaired t test. For assessment of change of a group by a certain intervention, the significance of data was assessed by the two-tailed paired t test. For comparison of multiple groups, one-way analysis of variance (ANOVA) with Dunnett's multiple comparison or Tukey post hoc test was assessed. For interaction between compartments/place (preferred vs. non-preferred) and tests (pre vs. post) as within-subject variables, and treatment groups as between-subjects variables, a repeated measures ANOVA was performed. For the electrophysiological experiment, Mini analysis (Synaptosoft) and Clampfit (Molecular Devices, MA, USA) were used. For plotting electrophysiological data, the Sigma plot (Systat, CA, USA) was used. A p-value of less than 0.05 was regarded as indicative of statistical significance throughout the study. Statistical significance was set at $^{*}p < 0.05$, $^{**}p < 0.01$, $^{***}p < 0.001$, $^{****}p < 0.0001$; ns, no significant. Data are presented as mean ± SEM. All experiments were conducted with a minimum of three biological replicates. Prior to the experiments, groups were balanced for animal age and body weight through appropriate pre-experimental grouping procedures. Animals were allocated to each experimental group using stratified randomization. To ensure blinded group allocation during data collection, animal preparation and the experiments were conducted by different investigators. The numbers and individual dots refer to the number of cells or animals unless otherwise clarified in the figure legends.